Electron impact excitation of the $a\,^3\Pi$, $a'\,^3\Sigma^+$, $d\,^3\Delta$ and $A\,^1\Pi$ states of CO at 10.0, 12.5 and 15.0 eV impact energies

1998 J. Phys. B: At. Mol. Opt. Phys. 31 2395

(http://iopscience.iop.org/0953-4075/31/10/025)

J. Phys. B: At. Mol. Opt. Phys. **31** (1998) 2395–2413. Printed in the UK PII: S0953-4075(98)88736-1

Electron impact excitation of the $a\,^3\Pi$, $a'\,^3\Sigma^+$, $d\,^3\Delta$ and $A\,^1\Pi$ states of CO at 10.0, 12.5 and 15.0 eV impact energies

P W Zetner†, I Kanik and S Trajmar

Jet Propulsion Laboratory, California Institute of Technology, Pasadena, CA 91109, USA

Received 27 October 1997, in final form 17 February 1998

Abstract. We have measured the differential and integral cross sections for electron impact excitation of the $a\,^3\Pi$, $a'\,^3\Sigma^+$, $d\,^3\Delta$ and $A\,^1\Pi$ states of CO in the 10–15 eV impact energy region. These measurements fill the gap which existed between the low-energy (threshold to about 12 eV) data of Zobel *et al* and the intermediate energy (20–50 eV) results of Middleton *et al*. Recent electron time-of-flight measurements are utilized to place the relative cross sections (deduced from energy-loss spectra) on the absolute scale.

The cross sections are in excellent agreement with the results obtained by Zobel *et al* at the overlapping impact energies and always smoothly extrapolate to their low-energy results. Extrapolation to the intermediate energy domain and comparison with the results of Middleton *et al* is not so clear.

Comparison with theoretical differential and integral cross sections of Sun *et al* and the integral cross sections of Morgan and Tennyson reveals angular and energy dependences which resemble those found for the experimental results but there are serious discrepances concerning the absolute magnitudes.

1. Introduction

Electron-impact excitation cross sections for CO are necessary to model various laboratory and industrial plasma systems (McDaniel and Nigham 1982). Electron impact excitation of CO also plays an important role in planetary atmospheres (Stewart 1972) and in stellar clouds (Dalgarno 1982). Cross section data available up to 1983 have been summarized by Trajmar *et al* (1983). For the low-lying valence states, considered here, several more recent measurements have been carried out. Middleton *et al* (1993) reported differential cross sections (DCSs) at 20, 30, 40 and 50 eV impact energies (E_0) at scattering angles (θ) ranging from 10° to 90° for excitation of the $a\,^3\Pi$, $a'\,^3\Sigma^+$, $A\,^1\Pi$ and the unresolved ($d\,^3\Delta + I\,^3\Sigma^- + I\,^1\Sigma^- + D\,^1\Delta$) states. Zobel *et al* (1996) measured DCSs for excitation of the $a\,^3\Pi$, $a'\,^3\Sigma^+$ and $A\,^1\Pi$ states for electron residual energies ranging from 0.2 to 2 eV and 0.2 to 3.7 eV in the 20–40° and 40–140° angular ranges, respectively. Le Clair *et al* (1996) deduced DCS values for 90° scattering angle at impact energies ranging from 6.5 to 15.0 eV for excitation of the $a\,^3\Pi$ state using a novel time-of-flight (TOF) approach. Recent theoretical works concerning excitation of these states are those of Sun *et al* (1992, 1996), Morgan and Tennyson (1993), and Lee *et al* (1996) based on the Schwinger multichannel variational, *R*-matrix, and distorted-wave methods, respectively.

The inelastic DCS measurements for CO (and for almost all atomic and molecular species), reported so far, have been obtained from conventional beam–beam scattering

† Permanent address: Department of Physics, University of Manitoba, Winnipeg, Canada.

0953-4075/98/202395+19$19.50

measurements. By conventional measurements here we mean measurements carried out with spectrometers utilizing electrostatic lenses and energy selectors with or without some corrections for instrument detection function. In these measurements relative scattering intensities for various excitation processes are extracted from energy-loss spectra. These relative intensities are assumed to be equal to the corresponding relative cross sections (or corrected for detection efficiency to some degree) and are then normalized to the absolute scale by measuring the inelastic-to-elastic scattering intensity ratios and utilizing known elastic DCS values. The problem with this procedure is that the instrument function is sensitive to the surface and tuning conditions of the apparatus and to the residual energy (E_R) of the scattered electron, especially at low residual energies and, therefore, the measured inelastic-to-elastic scattering intensity ratios do not, in general, represent the corresponding DCS ratios. To eliminate the dependence of electron detection efficiency on residual energy (E_R), one can utilize the isotropic nature of near-threshold ionization of He. This procedure can be applied at impact energies ranging from threshold to a few eV above threshold. The calibration can be extended to higher residual energies by assuming no residual energy dependence beyond these impact energies or by utilizing the known cross sections for excitation of the $n = 2$ and 3 manifolds and for elastic scattering. However, there is a remaining uncertainty associated with this procedure. The calibration of detector sensitivity has to be carried out with He at around 30 eV impact energy. The actual measurements are carried out with the sample gas and at other desired impact energies. Changing the gas (surface conditions) and the impact energy requires retuning of the spectrometer and this has an effect on the overall instrument function. Middleton *et al* (1993) utilized only the isotropic properties of He ionization and estimated the errors in the DCSs due to instrument function calibration to be about 10% at $E_0 \geqslant 20$ eV. Nickel *et al* (1989) described a calibration procedure utilizing both ionization and inelastic ($n = 2$ and 3 manifold excitation) and elastic scattering in He. They estimated the associated errors to be about 15% at similar impact energies. These procedures and the associated problems were discussed in detail by Nickel *et al* (1989), Allen (1992), Trajmar and McConkey (1994) and Le Clair *et al* (1996).

An elaborate technique was introduced very recently by Zobel *et al* (1996) which addresses and eliminates, in principle, all of these problems associated with the conventional cross section measurement method and represents a solution to the absolute calibration procedure. The drawbacks of this approach are the limit of applicability to the 0.2–3.7 eV residual energy range and the very time-consuming nature of the measurements.

A new approach in this area is represented by the work of Le Clair *et al* (1996). They applied electron TOF measurements to determine the scattering intensity ratios for certain inelastic transitions (usually several unresolved electronic transitions) and elastic scattering at fixed impact energies at 90° scattering angle. In this approach, the instrument function is shown to be independent of the residual energy of the electrons (in the range of $0.2 < E_R < 20$), and the intensity ratios represent the corresponding DCS ratios. Since the elastic DCS values are well established, the absolute inelastic DCSs can be reliably deduced for $\theta = 90°$. These inelastic DCS(90) values can then be used to normalize relative angular distributions of DCSs at the given impact energy for the same or nearby energy-loss processes.

We carried out extensive conventional measurements for electron-impact excitation of CO in the 10–20 eV impact energy and 4°–134° angular ranges and reported preliminary results at several conferences (Trajmar *et al* 1971, Zetner and Trajmar 1987, Zetner *et al* 1988). The DCS values obtained from these measurements were not published since our investigation concerning the calibration of the instrument function indicated that large (order of 30–50%) errors may be associated with this procedure. The errors are largest at around

10 eV impact energy for the CO states considered here since we are out of the near threshold region but the impact energies are not high enough to make the residual energy dependence of the detector negligible. Especially large error contributions come from the assumption that the inelastic-to-elastic scattering intensity ratios can be taken as the corresponding DCS ratios. In this paper, we utilize the results of these measurements to obtain *relative* DCS values for excitation of four valence states but achieve the normalization to the *absolute* scale by utilizing the DCS values obtained by Le Clair *et al* (1996) at $\theta = 90^\circ$ for excitation of the $a\,^3\Pi$ state from TOF measurements. DCSs are reported for these four states at 10.0, 12.5 and 15.0 eV impact energies in the 10°–140° angular range. These results fill the gap between the near threshold measurements of Zobel *et al* (1996) and those obtained by Middleton *et al* (1993) at $E_0 \geqslant 20$ eV. Furthermore, the TOF calibration method results in a smaller uncertainty in the absolute cross section values than those typically associated with the conventional measurement techniques.

2. Experimental procedures

The apparatus used for obtaining energy-loss spectra in the conventional beam–beam electron scattering measurements and the procedures for analysing these spectra to deduce the relative differential excitation cross sections have been described earlier (e.g. Cartwright *et al* 1977). Here we summarize only briefly the important points. The target CO beam was formed by effusing the gas through a capillary array with collimation $(L/2r)$ of 100 and back pressure of a few Torr. The electron impact spectrometer utilized electrostatic lens systems and double-hemispherical analysers both in the gun and the detector.

Energy loss spectra covering the elastic and 5.5–9.5 eV energy-loss regions were obtained at fixed impact energies of 10.0, 12.5 and 15.0 eV over the angular range of 4°–134° with about 40 meV resolution (FWHM). Energy loss spectra were obtained with the target beam ON and OFF. When the target beam was turned OFF, CO was admitted into the vacuum chamber to maintain the same background pressure. The background scattering was eliminated by subtracting the OFF spectrum from the ON spectrum.

In the second step, the resulting energy loss spectrum was corrected for the distortion caused by the variation of instrument function with energy loss. This correction was achieved by utilizing measurements of the ionization, excitation of the $n = 2$ and 3 manifold states and elastic scattering for He at 30.58 eV impact energy as described in detail by Nickel *et al* (1989). Typical energy-loss spectra, after these procedures, are shown in figures 1 and 2. The contributing electronic states and their vibrational structures are indicated and the energy-loss features are numbered from 1 to 19. (See table 1 for the assignment of these features in terms of the contributing transitions.)

In the third step, the undistorted energy-loss spectrum was unfolded into the contributing excitation processes by a least squares fitting procedure (see e.g. Cartwright *et al* 1977, Nickel *et al* 1989). At impact energies of 12.5 and 15.0 eV, we assumed that the Franck–Condon (FC) distribution was valid for the vibrational bands of each electronic state excitation and applied these factors as calculated by Cartwright (1972). Although there are noticeable deviations from FC factors in the intensity distribution among vibrational bands of a given electronic transition, these deviations nearly average out in summing over the whole band structure. To simplify our evaluation procedure at 15.0 and 12.5 eV impact energies, we considered the FC factors to be applicable in the unfolding procedure and incorporated the errors resulting from this assumption into the unfolding error. At these energies we carried out the unfolding with all seven electronic states $a\,^3\Pi$, $a'\,^3\Pi$, $d\,^3\Delta$, $e\,^3\Sigma^-$, $I\,^1\Sigma^-$, $A\,^1\Pi$ and $D\,^1\Delta$ and also with only four electronic states $a\,^3\Pi$, $a'\,^3\Pi$, $d\,^1\Delta$

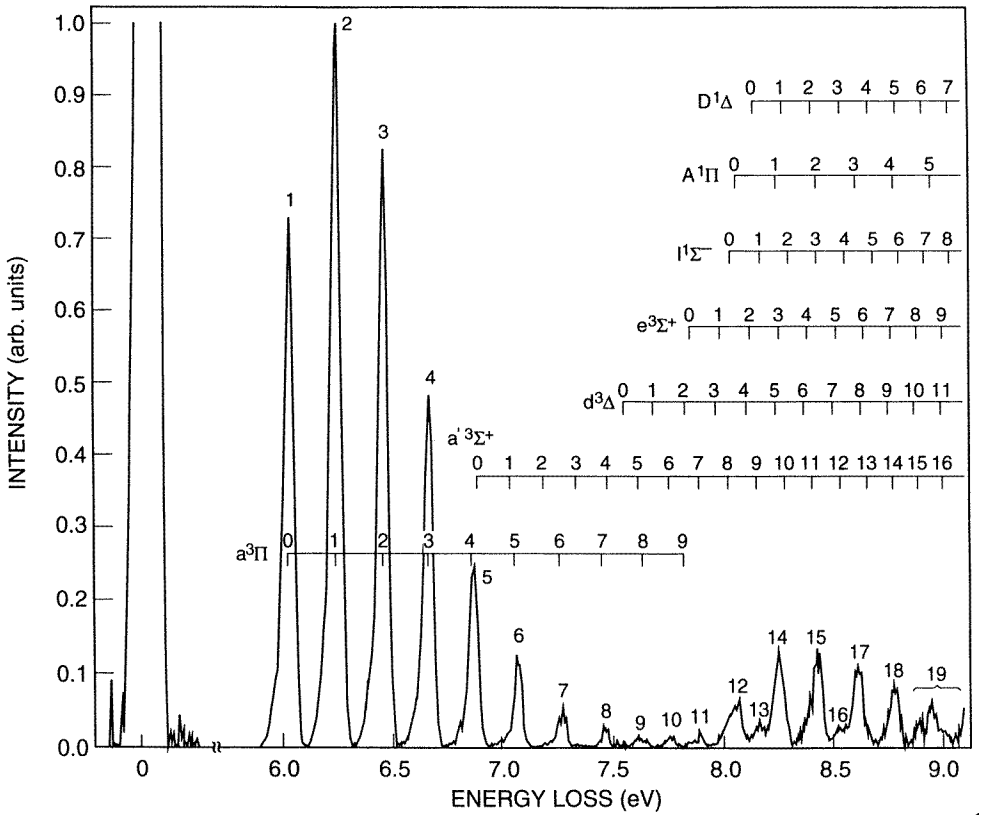

Figure 1. Energy-loss spectrum of CO at $E_0 = 10.0$ eV and $\theta = 93^\circ$. The vibrational band structure of the seven contributing states as well as the feature designation numbers are indicated.

and $A\,^1\Pi$ considered. In general, the $e\,^3\Sigma^-$, $I\,^1\Sigma^-$ and $D\,^1\Delta$ contributions were very small and highly uncertain. This fact is confirmed by the experimental observations of Zobel *et al* (1996). Theoretical calculations by Morgan and Tennyson (1993) concerning the integral cross sections for excitation of these seven electronic states indicate that the combined integral cross sections for the $e\,^3\Sigma^-$, $I\,^1\Sigma^-$ and $D\,^1\Delta$ states is about 20% of that of the $A\,^1\Pi$ state at 12.5 and 15.0 eV and less than 1% at 10.0 eV. The important point, however, is that for these three states the FC factors are distributed over a wide range of vibrational levels and reach their maximum value at $v > 12$ which corresponds to energy loss greater than 9.0 eV. Based on the integral cross sections, we, therefore, neglect contributions from these three states to the four states of interest to us (which are predominantly below 9.0 eV energy loss). We present the results for the fitting with four electronic states. The small contributions from the three neglected states are incorporated into the $a'\,^3\Sigma^+$, $d\,^3\Delta$ and $A\,^1\Pi$ state excitation intensities. At $E_0 = 10.0$ eV, we did not assume FC distributions and treated each feature in the energy loss spectrum as an individual transition.

From the results of the fitting procedure we calculated the inelastic-to-elastic scattering intensity ratios for the various transitions but *did not assume that these ratios were equal to the corresponding DCS ratios*. The intensity ratios combined with the known elastic DCS values yielded the inelastic DCS values *in arbitrary units* at each E_0 for groups of data taken under identical experimental conditions. If retuning of the spectrometer was

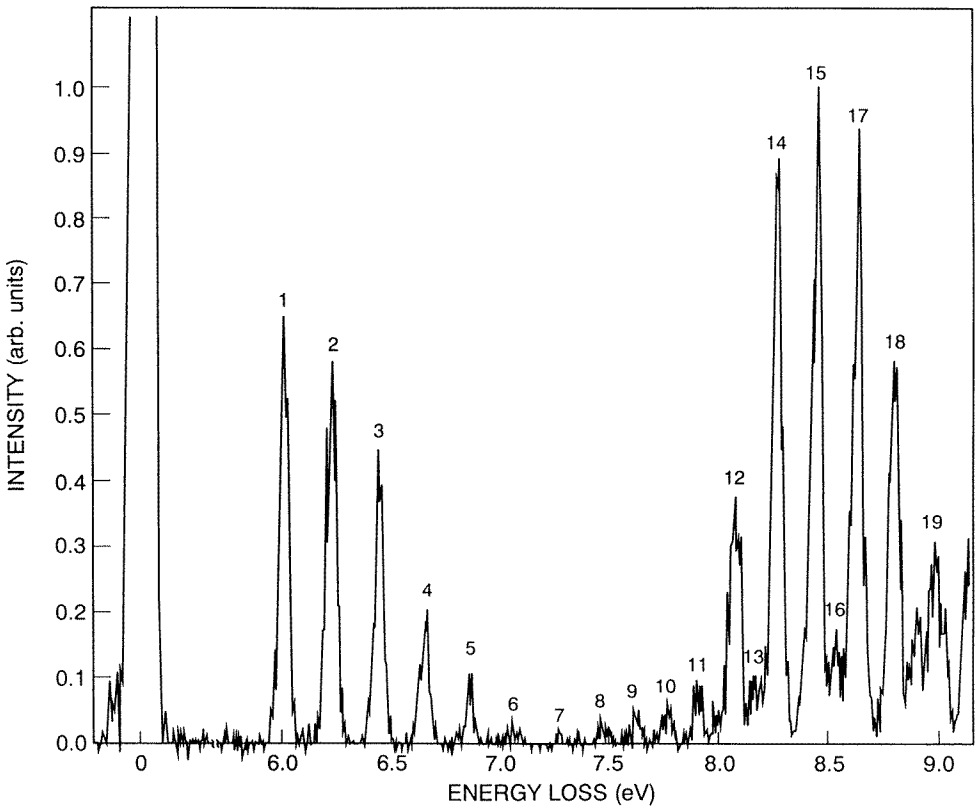

Figure 2. Same as figure 1, except $E_0 = 15.0$ eV and $\theta = 64^\circ$.

necessary, the data collected with the new tuning conditions were put into a new group so that each group contained data taken under identical experimental conditions. The elastic DCSs were measured by Tanaka *et al* (1978) based on calibration against He. Trajmar *et al* (1983) renormalized their elastic DCSs with improved He data. We used these renormalized values carrying out interpolations where necessary. It should be noted that these elastic cross sections include the rotationally inelastic transitions. More recently, Gote and Ehrhardt (1995) reported pure elastic and rotational excitation DCSs for CO at impact energies ranging from 10 to 200 eV. In the energy range of interest to us, they carried out these measurements only at 10 eV impact energy. The two sets of data are in good agreement in the 10–90° angular range but at angles 160° and higher they differ by about 20%. For consistency, we used the Tanaka/Trajmar results. Gibson *et al* (1995) supplied us with elastic DCSs for 90° scattering at $E_0 = 10.0$, 12.5 and 15.0 eV which are in excellent agreement with those of Tanaka/Trajmar.

The approach described above, to establish the angular distributions for the various excitation cross sections, was used to eliminate effective volume correction factors which relate the measured intensities to the corresponding DCSs and was considered more reliable than the alternate route of determining scattering intensity distributions and correcting them for change of scattering volume as well as making sure that the overlap conditions for the electron and CO beams and the view cone are constant over all angles.

In the fourth step, the inelastic DCS values obtained in arbitrary units for each group

Table 1. Assignment of features in the energy-loss spectra[a].

Feature number	Assignment							Energy-loss range (eV)
	$a\,^3\Pi$	$a'\,^3\Sigma^+$	$d\,^3\Delta$	$e\,^3\Sigma^-$	$I\,^1\Sigma^-$	$A\,^1\Pi$	$D\,^1\Delta$	
1	0							5.92–6.07
2	1							6.14–6.29
3	2							6.34–6.49
4	3							6.55–6.71
5	4	(0)						6.76–6.91
6	5	(2)						6.16–7.11
7	(6)	2 + 3						7.17–7.31
8	(7)	4						7.37–7.49
—	—	—	(0)					—
9	(8)	5	—					7.52–7.64
—	—	—	(1)					—
10	—	6	—					7.67–7.78
11	(9)	7	(2)	(0)				7.80–7.91
12	(10)	8	3 + 4	(1 + 2)	(0)	0		7.96–8.07
13	—	9	—	—	(1)	—	(0)	8.08–8.16
14	—	10	5	3	(2)	1	(1)	8.17–8.27
15	—	11	6	4	(3)	2	(2)	8.32–8.44
16	—	12	7	5	4	—	(3)	8.45–8.53
17	—	13	8	6	5	3	4	8.54–8.63
18	—	14	9	7	6	4	5	8.69–8.78
19	—	15 + 16	10 + 1	8 + 9	7 + 8	5	6 + 7	8.81–8.98

[a] The numbers under each heading specifying the electronic state refer to the vibrational quantum number. Numbers in parentheses indicate that contributions from these vibrational bands are negligible. Missing feature numbers mean that no feature from that band(s) is observable in the energy-loss spectra at the energy-loss location for that band(s).

of data were normalized to the absolute scale by the factor required to normalize the $a\,^3\Pi$ DCS(90) obtained from electron TOF measurement of each impact energy by Le Clair *et al* (1996). (Here, $a\,^3\Pi$ DCS(90) refers to the DCS for excitation of the $a\,^3\Pi$ state of CO at 90° scattering angle at the impact energy in question.) The assumption made here was that the correction factor applied to the $a\,^3\Pi$ excitation was the same for all inelastic transitions. This is a very good assumption under our experimental conditions.

The integral cross sections were obtained by extrapolating the DCSs to 0° and 180° and then integrating them over all angles. In the extrapolations we relied on the general trend and theoretical predictions.

For the estimation of experimental errors associated with these measurements, at 12.5 and 15.0 eV we considered error contributions from background subtraction (5%), the relative intensity measurement including unfolding procedure (typically 10–25%) and the normalization procedure including the errors associated with the DCS(90) values obtained from the TOF measurements for the excitation of the $a\,^3\Pi$ state (typically 12%). For the integral cross sections an additional error of about 5% is added due to extrapolation procedures. The overall errors are taken as the square root of the sum of the squares of the contributing errors. For the 10 eV results no unfolding errors are present. The estimated errors are 5% for background subtraction, 10–20% for the intensity measurements and 12% for the calibration to the TOF DCS(90°) value for the $a\,^3\Pi$ excitation. (The actual error limits are given together with the corresponding data in tables 2–4.) It should be noted that the inelastic angular distribution curves were derived from the elastic angular distribution

Table 2. Differential and integral cross sections at 15.0 eV impact energy[a].

Angle (deg)	DCS (10^{-18} cm^2 sr^{-1})			
	$a\,^3\Pi$	$a'\,^3\Sigma^+$	$d\,^3\Delta$	$A\,^1\Pi$
0	(0.90)	(1.90)	(3.75)	(52.0)
14	0.89	1.35	2.95	39.80
24	1.10	1.39	2.32	23.56
34	1.17	0.85	2.01	9.55
44	1.27	0.74	2.00	5.65
54	1.17	0.56	1.93	3.26
64	1.43	0.80	1.99	2.96
74	1.95	1.13	2.66	3.21
84	2.22	1.22	2.60	3.54
94	2.38	1.06	2.72	3.48
104	2.26	0.72	2.80	2.73
114	2.42	0.61	2.85	2.19
124	3.07	0.83	2.75	2.41
134	3.54	1.17	(2.80)	2.26
160	(3.90)	(2.2)	(2.70)	(2.25)
180	(3.70)	(2.8)	(2.50)	(2.20)
Error (%)	±16	±20	±28	±16
Q (10^{-18} cm^2)	28.45	13.06	32.02	64.95
Error (%)	±17	±21	±29	±17

[a] Values in parentheses are extrapolated values used to obtain the integral cross sections. All cross sections are for transitions from the ground $X\,^1\Sigma^+(v = 0)$ level to all vibrational levels of the indicated electronic state.

and were normalized to TOF at 90°. If the elastic angular distribution improves then the inelastic distribution will have to be corrected accordingly. This possible uncertainty was not considered in the error estimation.

3. Results and discussions

3.1. Differential cross sections at 15.0 and 12.5 eV

Features appearing in the energy loss spectra of CO in the 5.8–9.1 eV region correspond to excitations of the lowest seven valence electronic states and their vibrational levels (see figures 1 and 2). As discussed above, the scattering intensities associated with the $e\,^3\Sigma^-$, $I\,^1\Sigma^-$ and $D\,^1\Delta$ state excitations gave rise to very weak features in our spectra and could not be reliably determined. Based on our investigation (including analysis of spectra with seven-state unfolding procedures), we concluded that the contributions from these three states were mainly to the $A\,^1\Pi$ and $d\,^3\Delta$ excitations but represented only less than 5% of the scattering intensity associated with the $A\,^1\Pi$ state excitation. These contributions can be neglected, therefore, with respect to the $A\,^1\Pi$ state excitation but could be significant with respect to the $d\,^3\Delta$ state excitation. We analysed all energy loss spectra with the four-state unfolding procedure. In this analysis, it was assumed that the FC factors were applicable. Although this is not

Table 3. Differential and integral cross sections at 12.5 eV impact energy[a].

Angle (deg)	DCS (10^{-18} cm^2 sr^{-1})			
	$a\,^3\Pi$	$a'\,^3\Sigma^+$	$d\,^3\Delta$	$A\,^1\Pi$
0	(1.1)	(3.0)	(2.0)	(32.0)
9	1.17	2.51	2.68	26.52
14	1.30	2.23	1.58	20.68
24	1.45	2.18	2.11	14.25
39	1.80	1.12	1.81	6.18
44	1.82	1.09	1.78	4.98
54	2.17	0.82	2.52	3.63
69	2.51	0.69	1.96	2.50
84	3.14	0.89	1.58	2.29
94	3.55	0.83	1.65	2.34
99	3.78	0.91	1.94	2.76
114	4.78	0.84	1.83	2.44
129	5.29	0.77	1.66	2.15
134	5.23	0.69	1.48	1.91
Error (%)	±16	±20	±28	±16
Q (10^{-18} cm^2)	41.73	12.47	21.90	45.30
Error (%)	±17	±21	±29	±17

[a] DCS values in parentheses are extrapolated values used to obtain the integral cross sections. All cross sections are for transitions from the ground $X\,^1\Sigma^+(v = 0)$ level to all vibrational levels of the indicated electronic state.

strictly a valid assumption, it is true to a good approximation at 15.0 and 12.5 eV impact energies.

The differential cross sections and their error limits derived from the present measurements at 15.0 and 12.5 eV impact energies are given in tables 2 and 3 and are compared with other experimental and theoretical results in figures 3 and 4.

For the $a\,^3\Pi$ state excitation (to all vibrational levels), the present experimental DCSs and those calculated by Sun *et al* (1992) show similar qualitative behaviour with scattering angle but the theoretical values are about a factor of 2 larger than the experimental ones at both impact energies (figures 3(*a*) and 4(*a*)). The situation is similar for the excitation of the $a'\,^3\Sigma^+$ state. Both the experimental and the calculated DCSs exhibit similar oscillatory behaviour but again the theoretical results are about 50% larger (figures 3(*a*) and (*b*)). There are rather large uncertainties associated with the experimental DCSs for excitation of the $d\,^3\Delta$ state (figures 3(*c*) and 4(*c*)). The agreement between experiment and theory is, however, quite good both in angular behaviour and in magnitude. The DCSs for excitation of the $A\,^1\Pi$ state obtained from experiment and theory are in very good agreement both in angular behaviour and magnitude at angles larger than 40°. At lower angles, however, the strong forward peaking character appears only for the experimental DCSs. For this excitation process DCS values are also available from Zobel *et al* (1996) at 12.5 eV impact energy which are in excellent agreement with these results (figure 4(*d*)). The agreement between the two experimental data sets is very reassuring since they were obtained with different apparatus and by different normalization procedures.

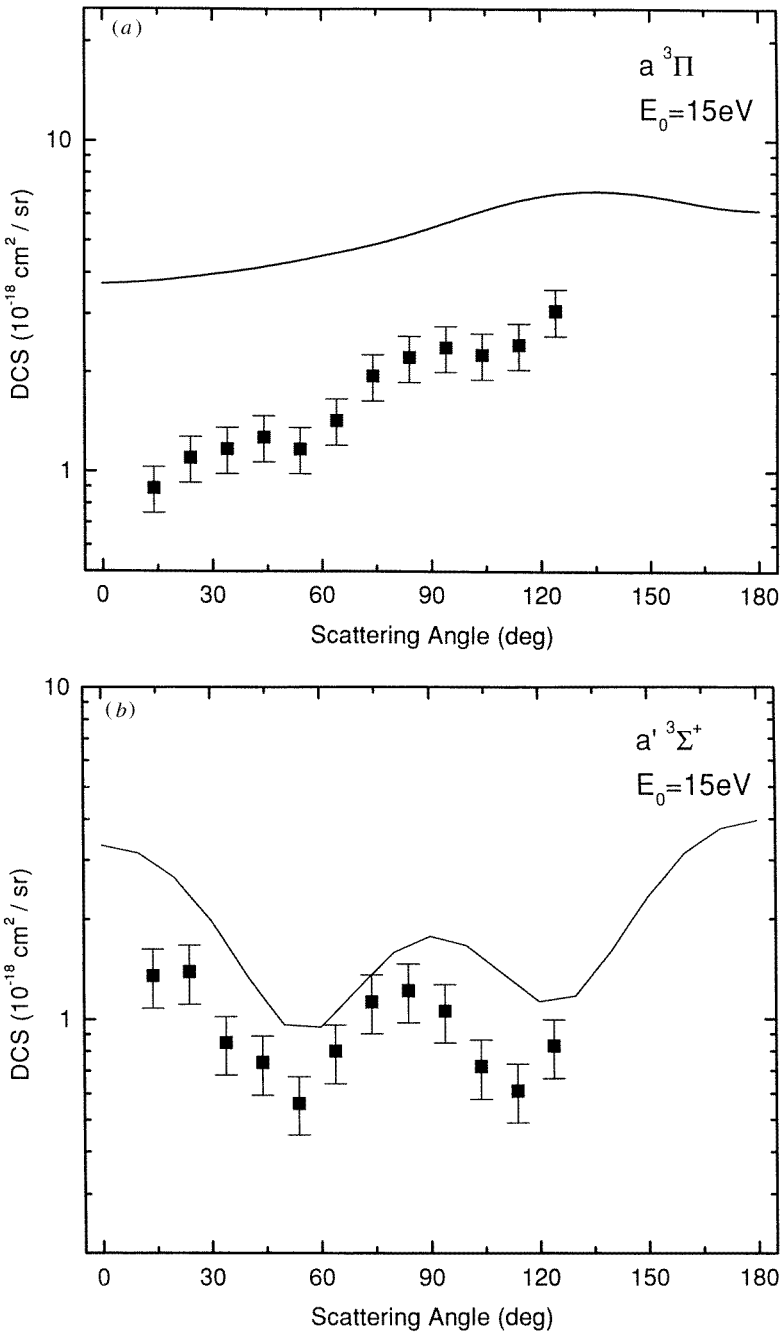

Figure 3. (*a*) Differential cross sections for excitation of the $a\,^3\Pi$ electronic state (for all vibrational levels) at $E_0 = 15.0$ eV. ■, present results; the full curve gives the theoretical results of Sun *et al* (1992). Typical error limits are indicated. (*b*) Same as (*a*) except for the $a'\,^3\Sigma^+$ state. (*c*) Same as (*a*) except for the $d\,^3\Delta$ state. (*d*) Same as (*a*) except for the $A\,^1\Pi$ state.

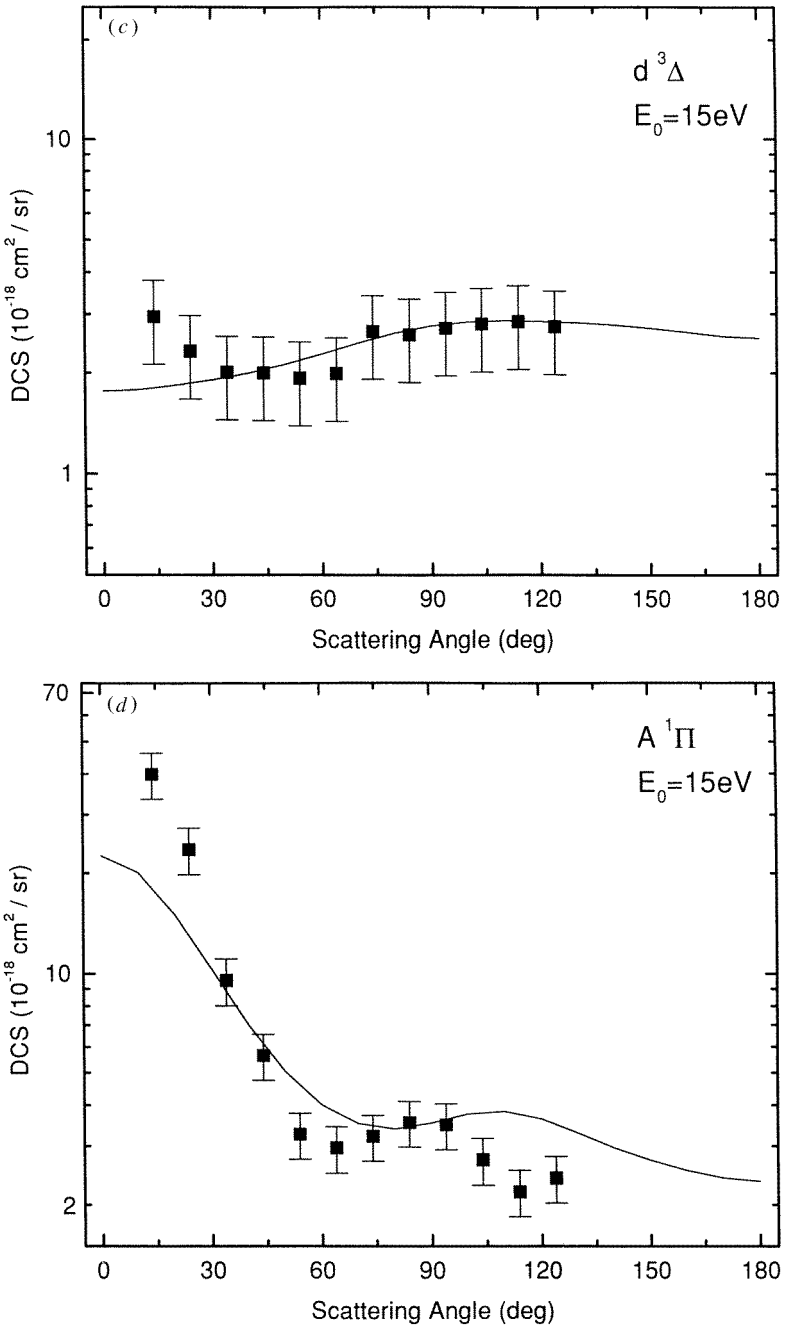

Figure 3. (Continued)

Table 4. Differential cross sections associated with features in the energy loss spectra of CO at 10.0 eV impact energy.

Feature	DCS (10^{-18} cm^2 sr^{-1})												
no	13°	23°	33°	43°	53°	63°	73°	83°	93°	103°	113°	123°	133°
1	0.774	0.813	0.833	0.879	0.946	1.109	1.206	1.44	1.601	2.028	2.175	2.491	2.13
2	1.033	1.066	0.093	1.169	1.201	1.461	1.614	1.89	2.230	2.777	2.892	3.449	2.85
3	0.784	0.805	0.834	0.885	0.971	1.119	1.228	1.49	1.781	2.159	2.228	2.580	2.16
4	0.395	0.440	0.460	0.520	0.593	0.649	0.717	0.85	1.049	1.234	1.276	1.527	1.26
5	0.183	0.217	0.228	0.267	0.330	0.325	0.361	0.42	0.530	0.596	0.614	0.714	0.62
6	0.115	0.106	0.121	0.142	0.169	0.156	0.145	0.18	0.232	0.222	0.242	0.299	0.25
7	—	0.0889	0.0585	0.0661	0.084	0.0661	0.081	0.069	0.101	0.0864	0.104	0.102	0.094
8	0.0927	0.0852	0.0584	0.0551	0.050	0.0503	0.038	0.039	0.0484	0.0401	0.049	0.0414	0.042
9	0.120	0.0964	0.0680	0.0540	0.050	0.0471	0.035	0.036	0.0353	0.0383	0.027	0.0416	0.040
10	0.170	0.106	0.107	0.0681	0.059	0.0476	0.041	0.036	0.0393	0.0341	0.041	0.0421	0.054
11	0.197	0.129	0.124	0.0919	0.063	0.0701	0.052	0.039	0.0485	0.0467	0.052	0.0564	0.067
12	0.942	0.726	0.626	0.427	0.413	0.292	0.256	0.22	0.189	0.222	0.299	0.286	0.23
13	0.348	0.196	0.222	0.143	0.117	0.0853	—	0.062	0.0883	0.0889	0.116	0.128	0.11
14	1.069	0.971	0.905	0.639	0.605	0.403	0.401	0.32	0.276	0.319	0.422	0.395	0.38
15	0.969	0.874	0.851	0.588	0.623	0.444	0.388	0.37	0.304	0.366	0.442	0.475	0.44
16	0.935	0.188	0.272	0.136	0.501	0.124	0.284	0.068	0.0689	0.0996	0.140	0.165	0.14
17	(0.6)	0.586	0.588	0.428	0.501	0.278	0.284	0.26	0.257	0.277	0.394	0.329	0.32
18	0.476	0.374	0.406	0.289	0.342	0.236	0.247	0.20	0.199	0.268	0.296	0.292	0.26
19a	0.433	0.384	—	0.115	0.300	0.0853	0.199	—	0.0645	0.276	0.347	0.250	0.23
19b	0.433	0.384	0.409	0.186	0.300	0.141	0.199	0.14	0.113	0.276	0.347	0.250	0.23

Errors: ±15% for DCSs $\geqslant 0.2 \times 10^{-18}$ cm^2 sr^{-1}. ±25% for DCSs $< 0.2 \times 10^{-18}$ cm^2 sr^{-1}.

3.2. Differential cross sections at 10.0 eV

Analysis of energy-loss spectra obtained at 10.0 eV impact energy could not be carried out in the same manner as at 12.5 and 15.0 eV since significant deviations from the FC distributions were present. Each spectral feature was, therefore, treated as an individual transition or combination of individual transitions as indicated in table 1. (No unfolding was applied and no FC distribution was assumed.) The DCS results are summarized in table 4 and comparisons with the experimental results of Zobel *et al* (1996) and with the calculations of Sun *et al* (1992) are shown in figures 5(*a*)–(*c*). Integral cross sections for excitation of the $a\,^3\Pi$ ($v = 0$–5), $a'\,^3\Sigma^+$ ($v = 6$, 7, 9) and $A\,^1\Pi$ ($v = 0$–4) states and indicated vibrational levels are shown in figures 6(*a*)–(*c*).

The DCS values for excitation of the $v = 0$–5 vibrational levels of the $a\,^3\Pi$ state are shown in figure 5(*a*). Excitations to higher vibrational levels appear very weak in the energy-loss spectra and are overlapped by other transitions. These six vibrational levels account for 99.8% of the excitation to all vibrational levels (based on FC factors). These results were obtained at $E_0 = 10.0$ eV, while those of Zobel *et al* (1996) were obtained at $E_R = 3.7$ eV (corresponding to $E_0 = 9.71$, 9.92, 10.13, 10.34, 10.54 and 10.74 eV for $v = 0$, 1, 2, 3, 4 and 5, respectively). The agreement between the two sets of data is excellent, well within the ±18 and ±24% error limits claimed in this work and by Zobel *et al* (1996), respectively. The theoretical results of Sun *et al* (1992) are about 50% larger than the experimental ones. In figure 5(*b*) the cross sections available for excitation of the $v = 6$, 7 and 9 vibrational levels of the $a'\,^3\Sigma^+$ electronic state are compared. Again, the experimental results of Zobel *et al* (1996) (obtained in the 60–140° range) and in this work (obtained in the 13–133° range) at $E_0 = 10.0$ eV are in excellent agreement. The

Table 5. Summary of differential and integral cross sections for excitation of selected vibrational levels in the $a\,^3\Pi$, $a'\,^3\Sigma^+$ and $A\,^1\Pi$ electronic states of CO at 10 eV impact energy[a].

		DCS (10^{-18} cm^2 sr)		
	Electronic state	$a\,^3\Pi$	$a'\,^3\Sigma^+$	$A\,^1\Pi$
	Vibrational levels	0–5	6, 7, 9	0–4
θ (deg)	Feature numbers	1–6	10, 11, 13	12, 14, 15, 17, 18
0		(3.20)	(0.95)	(4.3)
13		3.25	0.72	(4.0)
23		3.45	0.43	3.51
33		3.57	0.45	3.38
43		3.86	0.30	2.37
53		4.20	0.24	(2.28)
63		4.82	0.20	1.65
73		5.27	—	(1.59)
83		6.27	0.14	1.38
93		7.42	0.18	1.23
103		9.02	0.17	1.45
113		9.43	0.21	1.85
123		11.06	0.23	1.78
133		9.27	0.23	1.63
140		(11.30)	(0.24)	(1.75)
160		(11.45)	(0.24)	(1.75)
180		(11.50)	(0.24)	(1.75)
Error (%)		±16	±20	±16
Q (10^{-18} cm^2)		93.2	3.0	23.3
Error (%)		±17	±21	±17

[a] Numbers in parentheses were obtained by extrapolations or interpolations.

Table 6. Summary of present integral cross sections and associated Franck–Condon factors[a].

Excitation from $X\,^1\Sigma^+(v=0)$ to	Integral cross sections (10^{-18} cm^2) $E_0 = 10.0$ eV	$E_0 = 12.5$ eV	$E_0 = 15.0$ eV	FC
$a\,^3\Pi$ (v = 0–5)	93.2 ± 15.8	$[42.6 \pm 7.3]$	$[28.5 \pm 4.8]$	0.998
$a\,^3\Pi$ (all v)	$[93.2 \pm 15.8]$	42.6 ± 7.3	28.5 ± 4.8	1.000
$a'\,^3\Sigma^+$ (v = 6, 7, 9)	3.0 ± 0.5	$[2.4 \pm 0.5]$	$[2.4 \pm 0.5]$	0.184
$a'\,^3\Sigma^+$ (all v)	$[16.3 \pm 2.8]$	13.3 ± 2.8	13.1 ± 2.7	1.000
$A\,^1\Pi$ (v = 0–4)	23.3 ± 4.0	$[42.0 \pm 7.1]$	$[56.77 \pm 9.65]$	0.874
$A\,^1\Pi$ (all v)	$[26.6 \pm 4.5]$	48.0 ± 8.2	64.95 ± 11.04	1.000
$d\,^3\Delta$ (all v)	—	22.5 ± 6.5	32.0 ± 9.3	1.000

[a] FC refers to the Franck–Condon factors summed over the appropriate vibrational levels (from Cartwright 1972). The numbers in square brackets were derived from the measured values by using the appropriate FC factors.

$E_0 = 9.0$ eV results of Zobel *et al* (1996) are also shown to indicate the low-angle behaviour of their DCSs. The theoretical results of Sun *et al* (1992) for the excitation process are

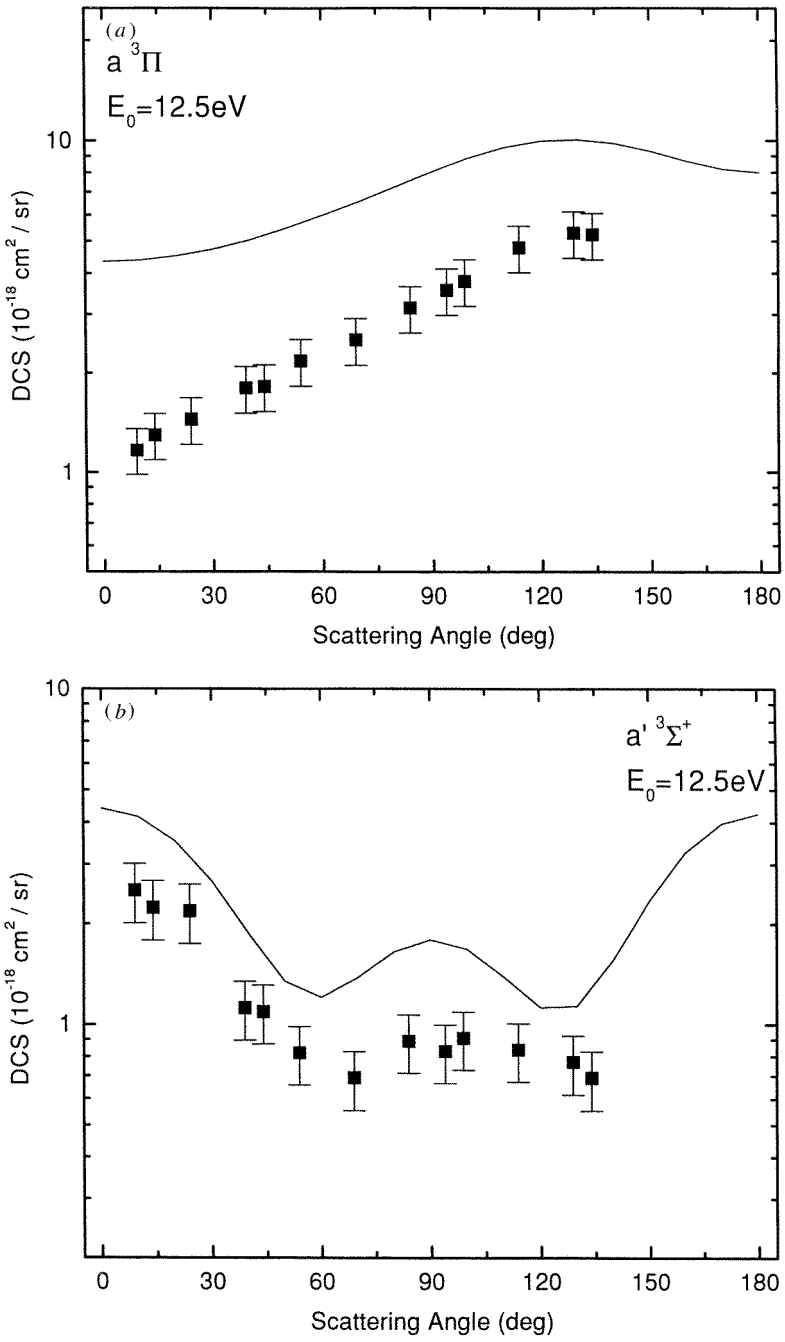

Figure 4. (*a*) Same as figure 3(*a*), except $E_0 = 12.5$ eV. (*b*) Same as (*a*) except for the $a'\,^3\Sigma^+$ state. (*c*) Same as (*a*) except for the $d\,^3\Delta$ state. (*d*) Same as (*a*) except for the $A\,^1\Pi$ state and in addition the results of Zobel *et al* (1966) are also given by the symbols △.

about a factor of 2 lower than the experimental ones and do not show the observed strong forward peaking character. The DCSs calculated by Sun *et al* (1992) for excitation of

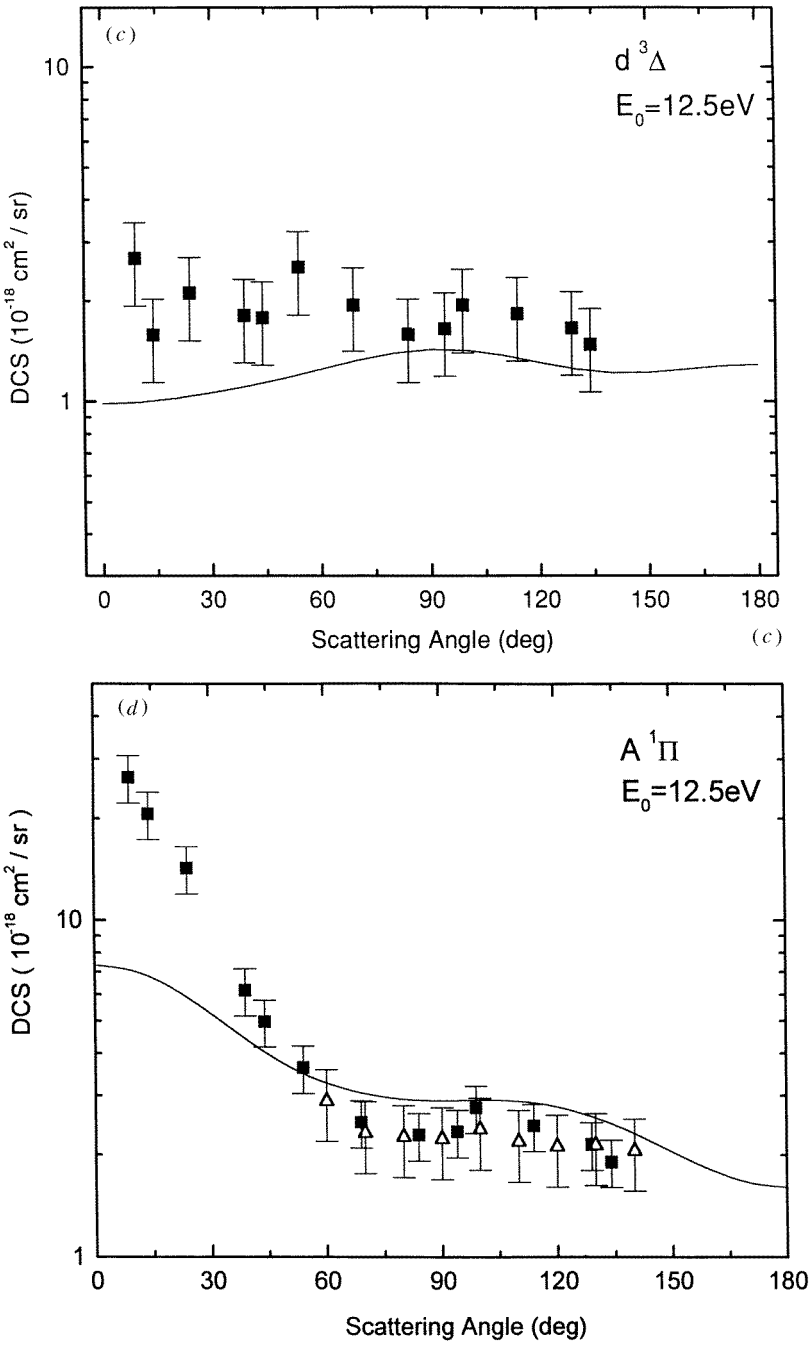

Figure 4. (Continued)

all vibrational levels were scaled down by a factor of 0.184 to correspond to the $a'^{3}\Sigma^{+}$ ($\nu = 6, 7, 9$) excitation. In figure 5(*c*) the DCSs for excitation of the $\nu = 0$–4 vibrational levels of the $A^{1}\Pi$ state are shown. These results are in excellent agreement with those

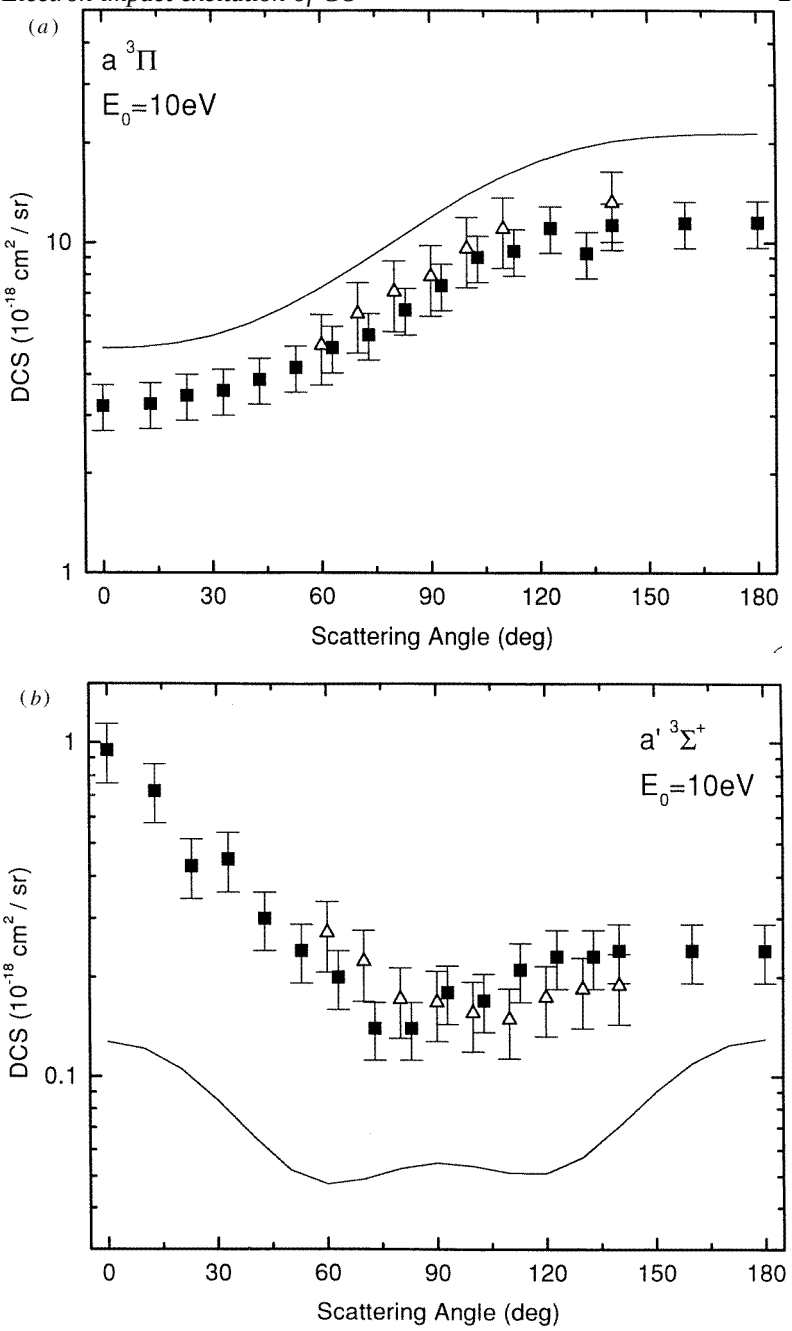

Figure 5. (*a*) Differential cross sections for the $X\,^1\Sigma^+$ ($v = 0$) $\rightarrow$ $a\,^3\Pi$ ($v = 0$–5) excitation process at $E_0 = 10.0$ eV. ■, present results and the full curve gives the theoretical results of Sun *et al* (1992). The experimental results of Zobel *et al* (1996) at constant residual energy of 3.7 eV are also given as △. Typical error limits are shown. (*b*) Same as (*a*), except for the $X\,^1\Sigma^+(v = 0) \rightarrow a'\,^3\Sigma^+$ ($v = 6, 7, 9$) excitation process and the theoretical results of Sun *et al* are at $E_0 = 10.5$ eV and scaled by a factor of 0.184. In addition, the values obtained by Zobel *et al* at $E_0 = 9.0$ eV are also shown as △. (*c*) Same as (*a*), except for the $X\,^1\Sigma^+(v = 0) \rightarrow A\,^1\Pi$ ($v = 0$–4) excitation process. The theoretical results of Sun *et al* are at $E_0 = 10.5$ eV and scaled by a factor of 0.847. The values of Zobel *et al* were obtained at constant residual energy of 1.8 eV.

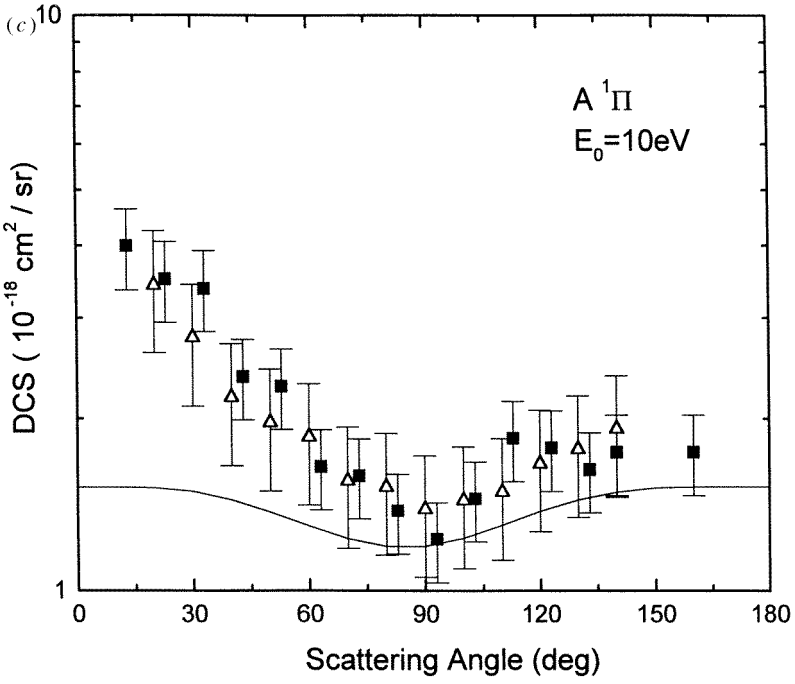

Figure 5. (Continued)

of Zobel *et al* (1996). The theoretical calculations (scaled again but by a factor of 0.874) show good agreement with experiment at angles larger than 60° but do not show the forward peaking observed in the experiments.

3.3. Integral cross sections

The differential cross section derived from these measurements were extrapolated to 0° and 180° scattering angles, guided by the qualitative behaviour of the theoretical results at high angles, and integrated to obtain the integral cross sections. These results are summarized in table 4 and compared with other results in figures 6(*a*)–(*c*).

For the $a^3\Pi$ ($v = 0$–5) excitation (figure 6(*a*)), Zobel *et al* (1996) obtained integral cross sections in the threshold to 9.5 eV impact energy range. These results were obtained at 10.0, 12.5 and 15.0 eV and represent a smooth continuation of the low-energy results. We also calculated the 20 and 30 eV values based on the measurements of Middleton *et al* (1993) in the 10–90° angular range and on our extrapolations to 0° and 180°. The value so obtained (and those which could be obtained by the same procedure from their 40 and 50 eV DCS results) extends the integral cross section curve to the higher impact energies. The consistency of these results give confidence in the measured values and establishes reliable integral cross sections from threshold to 50 eV impact energy. The theoretical cross section curves show similar behaviour to experiment but the calculated absolute values are considerably higher than the experimental ones.

The experimental results of Zobel *et al* (1996) and those obtained in this work are in excellent agreement both for the $a'^3\Sigma^+$ ($v = 6, 7, 9$) and the $A^1\Pi$ ($v = 0$–4) excitations (see figures 6(*b*) and (*c*)). Again, the integral cross sections obtained by us from the DCS

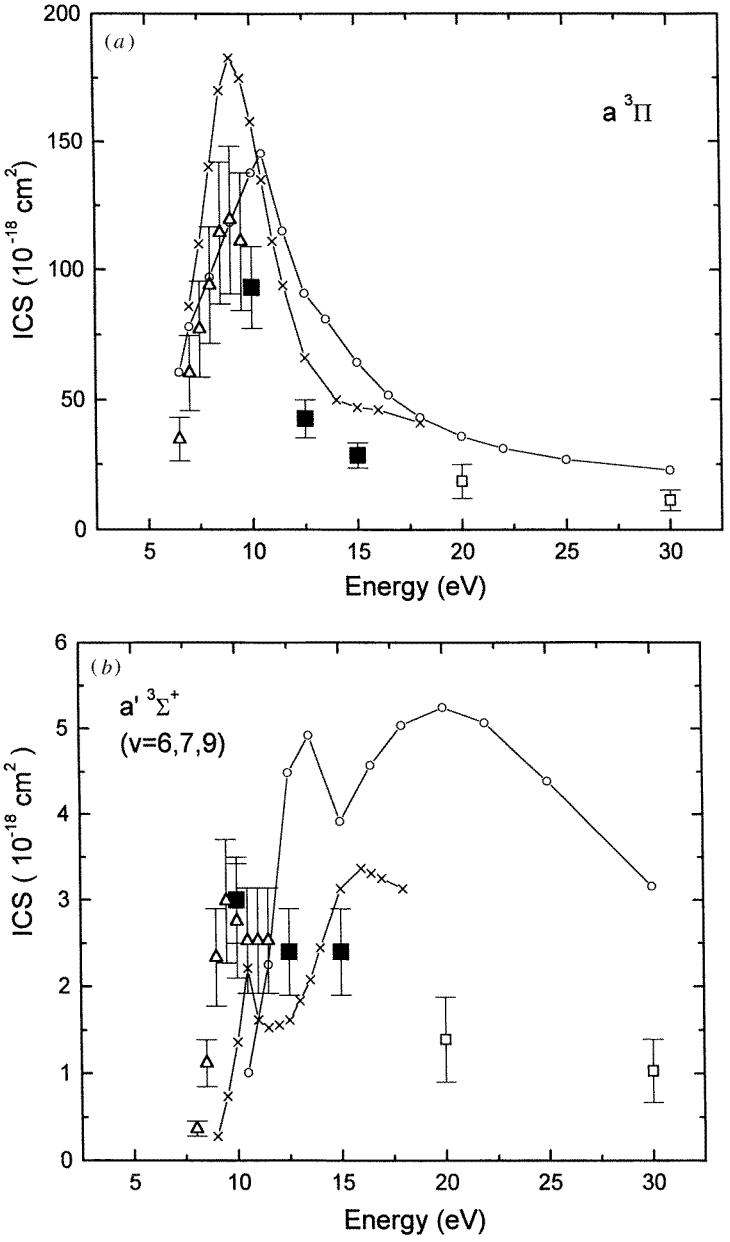

Figure 6. (*a*) Integral cross sections for $X\,^1\Sigma^+(v = 0) \rightarrow a'\,^3\Pi$ (all v) excitation process. Experimental results: ■, present; △, Zobel *et al* (1996); □, from the differential cross section measurements of Middleton *et al* (1993) integrated as described in the text. Theoretical results: (—○—), Sun *et al* (1992); (—×—) Morgan and Tennyson (1993). (*b*) Same as (*a*) except for the $X\,^1\Sigma^+(v = 0) \rightarrow a'\,^3\Sigma^+$ ($v = 6, 7, 9$) excitation process. (*c*) Same as (*a*) except for the $X\,^1\Sigma^+(v = 0) \rightarrow A\,^1\Pi$ ($v = 0$–4) excitation process.

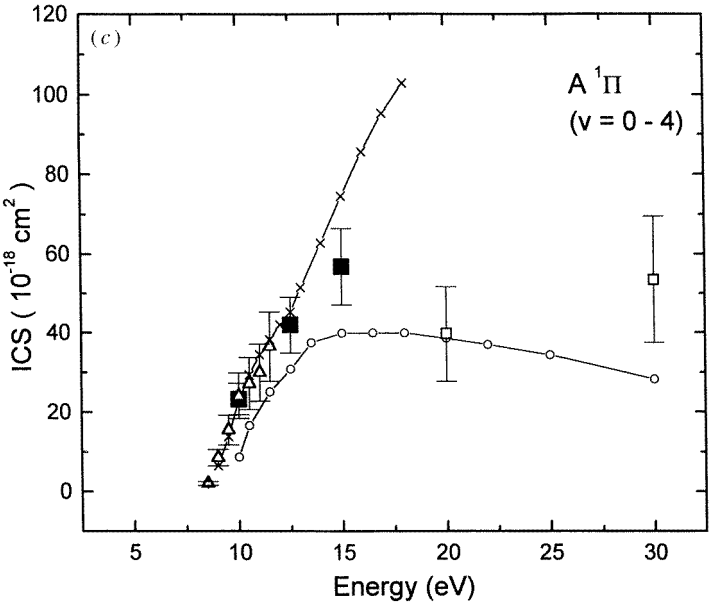

Figure 6. (Continued)

results of Middleton *et al* (1993) at 20 and 30 eV impact energies are also shown. These results complement those obtained by Zobel *et al* (1996) and extend the integral cross section behaviour up to $E_0 = 15.0$ eV. The extrapolation to $E_0 = 20$ eV to connect these results with those deduced from the DCS values of Middleton *et al* (1993) in the 20–50 eV impact energy range is somewhat uncertain for both the $a'\,^3\Sigma$ and $A\,^1\Pi$ excitations. It also has to be kept in mind that due to the limited angular range (10°–90°) of the Middleton *et al* (1993) DCSs, the derived integral cross sections are associated with large uncertainties ($\sim \pm 35\%$). Within these large uncertainties, the higher energy integral cross sections for the $a'\,^3\Sigma$ case are not inconsistent with the low-energy data. For the $A\,^1\Pi$ excitation, however, the situation is rather puzzling (see figure 6(*c*)). The theoretical results are not consistent with experiments either in magnitude or in their energy dependence.

The integral cross sections obtained in this work and by Zobel *et al* (1996) for the $d\,^3\Delta$ excitation have too large error limits for meaningful comparisons. Comparison of the integral cross sections to optical excitation functions and metastable production cross sections are given by Zobel *et al* (1996).

4. Summary and conclusions

The differential and integral cross sections reported here for electron impact excitation of the $a\,^3\Pi$, $a'\,^3\Sigma^+$, $d\,^3\Delta$ and $A\,^1\Pi$ states of CO in the 10–15 eV impact energy region fill the gap which existed between the low-energy (threshold to about 12 eV) data of Zobel *et al* (1996) and the intermediate energy (20–50 eV) results of Middleton *et al* (1993). Recent electron TOF measurements (Le Clair *et al* 1996) were utilized in this work to place the relative cross sections (deduced from energy-loss spectra) on the absolute scale. We consider this approach to be more reliable and practical than other normalization methods.

These cross sections are in excellent agreement with the results obtained by Zobel *et al*

(1996) at the overlapping impact energies and always smoothly extrapolate to their low-energy results. Extrapolation to the intermediate energy domain and comparison with results of Middleton *et al* (1993) is not so clear. Excellent smooth joining curves exist for the $a\,^3\Pi$ integral excitation cross sections, reasonable consistency (within error limits) is found for the $a'\,^3\Sigma^+$ excitation. The situation concerning the $A\,^1\Pi$ excitation is not as good, but the experimental results could be consistent within the error limits. The theoretical results exhibit angular and energy dependences which resemble those found for the experimental results but there are serious discrepancies concerning the absolute magnitudes of the cross sections. It is clear that the theoretical methods require further improvements and cannot be relied on at the present time.

Acknowledgments

The authors wish to express their gratitude to V McKoy, J Zobel and J C Gibson for valuable discussions and for supplying their results in a tabulated form. We also wish to thank L Le Clair for help and discussions concerning the TOF calibration. This work was carried out at the Jet Propulsion Laboratory, California Institute of Technology and was supported by the National Aeronautics and Space Administration and by the National Science Foundation.

References

Allen M 1992 *J. Phys. B: At. Mol. Opt. Phys.* **25** 1559
Ayres T R, Moos H W and Lynsky J L 1981 *Astrophys. J.* **248** L137
Cartwright D C 1972 Private communication to be published
Cartwright D C, Williams W, Trajmar S and Chutjian A 1977 *Phys. Rev.* **16** 1041
Dalgarno A 1982 *Applied Atomic Collision Physics* vol 1 (New York: Academic) pp 427–67
Gibson J C, Morgan L, Gulley R J, Brunger M J and Buckman S J 1996 *J. Phys. B: At. Mol. Opt. Phys.* **29** 3197
Gote M and Ehrhardt H 1995 *J. Phys. B: At. Mol. Opt. Phys.* **28** 3957
Le Clair L R, Trajmar S, Khakoo M A and Nickel J C 1996 *Rev. Sci. Instrum.* **67** 1753
Lee M T, Machado A M, Fujimoto M M, Machado L E and Brescansin L M 1996 *J. Phys. B: At. Mol. Opt. Phys.* **29** 4285
McDaniel E W and Nigham W L 1982 *Applied Atomic Collision Physics Vol. 3 Gas Lasers* (New York: Academic) pp 118–29
Middleton A G, Brunger M J and Teubner P J O 1993 *J. Phys. B: At. Mol. Opt. Phys.* **26** 1743
Morgan L A and Tennyson J 1993 *J. Phys. B: At. Mol. Opt. Phys.* **26** 2429
Nickel J C, Zetner P W, Shen G and Trajmar S 1989 *J. Phys. E: Sci. Instrum.* **22** 730
Stewart A I 1972 *J. Geophys. Res.* **77** 54
Sun Q, Winstead C and Mc Koy V 1992 *Phys. Rev.* A **46** 6987
——1996 Private communication
Tanaka H, Srivastava S K and Chutjian A 1978 *J. Chem. Phys.* **69** 5329
Trajmar S and McConkey J W 1994 *Adv. At. Mol. Opt. Phys.* **33** 63
Trajmar S, Register D F and Chutjian A 1983 *Phys. Rep.* **97** 219
Trajmar S, Williams W and Cartwright D C 1971 *VIIth Int. Conf. on the Physics of Electronic and Atomic Collisions (Amsterdam)* (Amsterdam: North-Holland) Abstracts p 1056
Zetner P W, Kanik I, Nickel J C and Trajmar S 1988 *41st Gaseous Electronics Conf. (Minneapolis, MN)* Book of Abstracts p 119
Zetner P W and Trajmar S 1987 *XVth Int. Conf. on the Physics of Electronic and Atomic Collisions (Brighton)* (Amsterdam: North-Holland) Abstracts of Contributed papers p 307
Zobel J, Mayer U, Jung K and Ehrhardt H 1996 *J. Phys. B: At. Mol. Phys.* **29** 813
——1996 private communication